JOURNAL OF THERMOPHYSICS AND HEAT TRANSFER
Vol. 14, No. 4, October–December 2000

Friction Factor and Nusselt Number for Thermoacoustic Transport Phenomena in a Tube

Guoqiang Lu* and Ping Cheng†
Hong Kong University of Science and Technology, Hong Kong, People's Republic of China

The transport phenomena for a viscous compressible oscillating flow (with a zero mean velocity) in a tube subjected to a prescribed cycle-steady axial temperature gradient are analyzed. The governing equations are linearized under the conditions of high oscillating frequencies, small amplitudes, and in a tube with a high length-to-radius ratio. Based on a linearized theory, an analytical expression is obtained for the local friction factor, which depends on the prescribed cycle-steady axial temperature and independent of time. The local friction factor is shown to be a complex number indicating a phase shift between the cross-sectional averaged velocity and the local pressure gradient. Closed-form analytical expressions are also obtained for the temperature distribution and for the Nusselt number of solid/fluid interfacial heat transfer by solving the energy equations of the fluid and solid phases. The Nusselt number is also a complex number indicating a phase shift between the heat flux and the temperature difference between the wall and the oscillating fluid. The magnitude of the Nusselt number is also dependent on the prescribed axial cycle-steady temperature and independent of time, and is related to dimensionless thermal property parameters, dimensionless geometrical parameter, and dimensionless operation conditions parameters. To understand the momentum transport and energy transport characteristics, the radial distributions of axial velocity and temperature of the fluid are presented for different ratios of the inner radius with respect to fluid's viscous penetration depth. Particular attention is given to the transport phenomena in the following two limiting cases: 1) a viscous compressible oscillating flow in a porous medium based on a capillary-tube model, and 2) a viscous compressible oscillating flow in a resonant tube of a thermoacoustic refrigerator or in a pulse tube of a Stirling-type pulse-tube refrigerator.

Nomenclature

A	=	cross-sectional area
a	=	local speed of sound
C_p	=	thermal capacity
f	=	friction factor
h	=	interfacial heat transfer coefficient
i	=	unit complex number
$J_j(\eta)$	=	Bessel function of the first kind of order j
k	=	thermal conductivity
L	=	length
Nu	=	Nusselt number
Pr	=	Prandtl number
p	=	pressure
R	=	gas constant
R_i	=	inner radius
R_o	=	outer radius
r	=	radial coordinate
s	=	amplitude of motion
T	=	temperature
u	=	axial velocity
v	=	radial velocity
x	=	axial coordinate
$Y_j(\eta)$	=	Bessel function of the second kind of order j
α	=	thermal diffusivity
γ	=	ratio of specific heats
Δ	=	R_o/R_i
δ_ν	=	fluid's viscous penetration depth
ε	=	$k_{s,0}\sigma_s/k_0\sigma$
η_0	=	$(i-1)R_i/\delta_\nu$
μ	=	viscosity
ν	=	kinematic viscosity
ρ	=	density
σ	=	$(\nu_0/\alpha_0)^{1/2}$, $Pr^{1/2}$
σ_s	=	$(\nu_0/\alpha_{s,0})^{1/2}$
ϕ	=	$(a/\omega L)^2(1/T_0)(\mathrm{d}T_0/\mathrm{d}x)(1/p)(\partial p/\partial x)$
Ω	=	certain physical quantity
ω	=	angular velocity

Subscripts

d	=	amplitude
s	=	solid
0	=	cycle average
1	=	first harmonic order

Superscripts

-	=	cross-sectional average
*	=	dimensional quantities

Introduction

RECENTLY, renewed interest has been given to the study of thermoacoustic refrigerators and pulse-tube refrigerators because these devices use non-chlorofluorocarbon (CFC) refrigerants that are environmentally benign. Such a device usually consists of several components in series: a pressure waves generator, a porous medium regenerator, a cylindrical void tube, two heat exchangers, and a reservoir. The viscous compressible oscillating flow in these devices is generated by the pressure wave generator. As a result of the periodic expansion and compression of the gas, the temperature at the cold-end heat exchanger gradually decreases until a specific longitudinal cycle-average temperature gradient is established, which is identified as a cycle-steady condition. Experiments show that there is a specific cycle-steady temperature gradient for a given geometry of the refrigerator at a given set of operating conditions.[1,2] We will call this specific longitudinal cycle-average temperature gradient as the cycle-steady temperature gradient in this paper.

The linearized theory[3–5] has been used in most of the early work on the study of the thermoacoustic transport phenomena in a tube

Received 29 November 1999; revision received 25 May 2000; accepted for publication 31 May 2000. Copyright © 2000 by the American Institute of Aeronautics and Astronautics, Inc. All rights reserved.

*Research Assistant, Department of Mechanical Engineering, Clear Water Bay, Kowloon.

†Professor and Head, Department of Mechanical Engineering, Clear Water Bay, Kowloon. Associate Fellow AIAA.

or between two parallel plates. For these problems with simple and fixed boundary conditions, analytical solutions are possible. In the pioneering work of Rott,[3,4] the governing equations for an axisymmetric viscous compressible oscillating flow are linearized for the case of high oscillating frequencies, with small oscillation amplitudes in a long tube with a prescribed axial temperature gradient. He obtained analytical solutions for radial distributions of velocity and temperature for such a viscous compressible oscillating flow in a tube. Swift[5] presented an extensive review on thermoacoustic machines and extended Rott's[3,4] thermoacoustic theory by considering the conjugate heat transfer problem in the fluid as well as in the solid. Based on Rott's[3,4] and Swift's[5] linearized theory, Xiao[6] obtained analytical solutions for velocity and temperature distributions of a two-dimensional viscous compressible oscillating flow in a tube and between parallel plates with different thermal boundary conditions on the outer surface of the wall.

To study the performance of a thermoacoustic machine consisting of several heat transfer components in series and with axial boundary conditions between different components coupled and unknown, it is more convenient to use a transient one-dimensional numerical model. In these transient one-dimensional models, however, correlation equations of the friction factor and the interfacial heat transfer coefficient for a viscous compressible oscillating flow must be known a priori. In this connection, note that the correlation equations for the friction factor and the heat transfer coefficient in a regenerator obtained by Kays and London[7] and Tanaka et al.[8] were based on measurements of a steady unidimensional flow. If these correlation equations were used for the numerical simulation of an oscillating flow in a thermoacoustic machine, it would lead to serious errors because the phase shifts of the friction factor and heat transfer coefficient with respect to the velocity, due to transient effects, are not taken into consideration. In a recent paper, Watanabe et al.[9] performed an analysis on oscillating viscous compressible flow between parallel plates. They assumed that the interfacial heat transfer consisted of two heat transfer operators: one due to the axial temperature gradient and the other due to a difference between the wall temperature and the fluid temperature of the oscillating flow. Based on a linearized theory, they obtained an analytical expression for the interfacial heat transfer.

In this paper, analytical solutions for the friction factor and the interfacial Nusselt number of a viscous compressible flow oscillating at high frequencies in a tube, subjected to a prescribed cycle-steady axial temperature gradient, are obtained based on the first-order linearized equations. The conventional definition of solid/fluid interfacial heat transfer coefficient is adopted here, which differs from that of the work of Watanabe et al.[9] We chose to study a cylindrical configuration because most of thermoacoustic machines are of cylindrical shape, and the porous medium regenerators in these machines can be simplified by a capillary-tube model. The friction factor of such a viscous compressible oscillating flow in a long tube is obtained. It is shown that the friction factor is a complex number because of the phase shift between the cross-sectional velocity and pressure gradient. Its magnitude depends on the prescribed cycle-steady temperature because the viscosity is a function of temperature. An analytical expression of the Nusselt number for the solid/fluid interface is obtained by solving the first-order conjugate heat transfer problem in the fluid and the solid phases. The friction factor and the Nusselt number presented in this paper can be used for the numerical simulation of the performance of a thermoacoustic machine using a transient one-dimensional model.

It should be emphasized that the results of the present work are not applicable to a viscous compressible flow oscillating at a low frequency with large pressure fluctuations, where the assumptions of the thermoacoustic theory are not valid. For this case, one may refer to the work by Bauwens,[10] in which a perturbation solution valid for a two-dimensional viscous compressible flow, oscillating at a low frequency with large fluctuations, is obtained.

Physical Model

We now study the transport phenomena of a viscous compressible flow oscillating in a cylindrical tube with a length L having an outer radius of R_o and an inner radius of R_i as shown in Fig. 1. We consider the case where the outside of the cylindrical tube is insulated and there exists a cycle-steady axial temperature gradient in the fluid and solid due to the periodic expansion and compression of the compressible oscillating flow, which occurs in a thermoacoustic machine as mentioned in the previous paragraph. The governing equations for an axisymmetric viscous compressible flow in a tube are the continuity equation, Navier–Stokes equations in the axial and the radial directions, and energy equations for the fluid and the solid, as well as the state equation. The linearization of the governing equations for a viscous oscillatory compressible flow was discussed by Swift,[5] and we will not repeat it here. However, to make this paper self-contained, we will state the assumptions made in the following analysis.

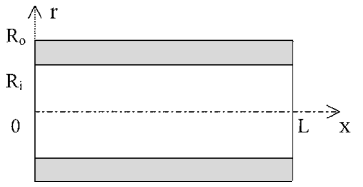

Fig. 1 Schematic diagram.

Assumption 1: The oscillating frequency of the flow is high, and the wavelength of the oscillating flow is much smaller than the tube length so that the percentage change of the absolute temperature over the amplitude of the motion is small. As discussed by Rott,[4] this assumption is valid if oscillating amplitudes of physical quantities are small, and $s(\mathrm{d}\log T_0/\mathrm{d}x) \ll 1$, where $T_0(x)$ is the prescribed cycle-average temperature. This assumption is applicable in a thermoacoustic machine because it is always operated at a near resonant frequency with small oscillating amplitudes. This assumption is also applicable to a Stirling-type pulse-tube refrigerator operating at high frequencies.

Assumption 2: The tube is long such that $L \gg R_o > R_i$. Under this assumption, we can neglect the viscous effect due to axial velocity gradient in the axial Navier–Stokes equation based on an order of magnitude analysis. Similarly, we can neglect the axial heat conduction terms in the energy equations for the fluid and the solid compared to the radial heat conduction terms. In addition, work by viscous forces can also be neglected in the fluid energy equation. Furthermore, the radial momentum equation can be neglected, and the pressure can be considered to be independent of radial coordinate, that is,

$$\frac{\partial p}{\partial r} = 0 \tag{1a}$$

or

$$p = p(x, t) \tag{1b}$$

where t is the time coordinate. Note that Eqs. (1a) and (1b) are of the same form as those in the boundary layer theory.

Assumption 3: To simplify the problem, we follow the previous studies[3–6] by assuming that the cycle-average oscillating velocity of the fluid equals to zero. Thus, we take $u_0 = 0$ and $v_0 = 0$.

We now decompose all of the physical quantities into time-average quantities and time-varying quantities as

$$\Omega(x, r, t) = \Omega_0(x, r) + \Omega_1(x, r, t) + \cdots \tag{2a}$$

where Ω is a certain physical quantity such as temperature, pressure, velocity, density, or other thermal property, with the subscript 0 denoting the zero-order quantity and the subscript 1 the first-order harmonic quantity, the latter of which is small in comparison with the zero-order quantity according to the first assumption. We now substitute the physical quantities given by Eq. (2a) into the governing equations, and neglect the high-order quantities due to their small orders. This leads to the following zero-order equations:

$$\frac{\partial p_0}{\partial x} = 0 \tag{2b}$$

$$p_0 = R\rho_0 T_0 \tag{2c}$$

$$k\frac{\partial^2 T_0}{\partial r^2} = k_s\frac{\partial^2 T_{s,0}}{\partial r^2} = 0 \tag{2d}$$

where k and k_s are the thermal conductivities of the fluid and solid, respectively, which are temperature dependent. Equation (2b) is obtained by substituting Eq. (2a) into the axial momentum equation, which indicates that the mean pressure is a constant independent of axial and radial positions. Equation (2c) is derived from the state equation, and Eq. (2d) is from the energy equations. Moreover, by substituting Eq. (2a) into the radial boundary condition of the temperatures, we have

$$r = R_i: \qquad k\frac{\partial T_0}{\partial r} = k_s\frac{\partial T_{s,0}}{\partial r} \tag{2e}$$

$$T_0 = T_{s,0} \tag{2f}$$

$$r = R_o: \qquad \frac{\partial T_{s,0}}{\partial r} = 0 \tag{2g}$$

From Eqs. (2d–2g), we have

$$T_0 = T_{s,0} \tag{2h}$$

$$\frac{\partial T_0}{\partial r} = \frac{\partial T_{s,0}}{\partial r} = 0 \tag{2i}$$

Therefore, a further simplification can be made to the zero-order quantities, such as temperatures, pressure, and density, which are independent of time and are also independent of radial position. The determination of $T_0(x)$ analytically is beyond the scope of the present study. In the following, we will assume that $T_0(x)$ is prescribed.

The first-order equations are of particular interest in the present work. As a result of the first assumption indicating that the acoustic wavelength of the oscillating flow is much smaller than the tube length, we can neglect the convective terms $u_1(\partial u_1/\partial x)$ and $v_1(\partial u_1/\partial x)$ compared to the transient term $\partial u_1/\partial t$ in the first-order axial momentum equation based on an order of magnitude analysis. However, the case of the first-order fluid energy equation is somewhat different due to the existence of a large axial cycle-steady temperature gradient. Thus, the term $u_1(\mathrm{d}T_0/\mathrm{d}x)$ should not be neglected, although we can neglect terms $u_1(\partial T_1/\partial x)$ and $v_1(\partial T_1/\partial x)$ compared to the transient term $\partial T_1/\partial t$ similar to the case in the first-order axial momentum equation. As a result, the first-order equations are further simplified. The resulting equations can be expressed in a dimensionless form by scaling the radial coordinate by the inner radius R_i, axial coordinate by the tube length L, time by the $1/\omega$, temperature by the local cycle-average temperature $T_0(x)$, pressure by the local cycle-average pressure $p_0 = R\rho_0 T_0$, and velocity by the local speed of sound $a = \sqrt{(\gamma R T_0)}$, where ω is frequency. Suppose that the first-order harmonic quantities are of the form $\Omega_1(x, r, t) = \Omega_d(x, r)e^{i\omega t + i\vartheta}$, where ϑ is a phase angle, then we have $\partial\Omega_1/\partial t = iw\Omega_1$. This leads to the following dimensionless first-order equations:

$$i\rho + \frac{a}{\omega R_i}\frac{1}{r}\frac{\partial}{\partial r}(vr) + \frac{1}{\omega L\rho_0}\frac{\partial}{\partial x}(au\rho_0) = 0 \tag{3}$$

$$iu = -\frac{a}{\omega L\gamma}\frac{\partial p}{\partial x} + \frac{\nu_0}{\omega R_i^2}\frac{1}{r}\frac{\partial}{\partial r}\left(r\frac{\partial u}{\partial r}\right) \tag{4}$$

$$iT + \frac{a}{\omega L}\frac{1}{T_0}\frac{\mathrm{d}T_0}{\mathrm{d}x}u = \frac{\gamma - 1}{\gamma}ip + \frac{\alpha_0}{\omega R_i^2}\frac{1}{r}\frac{\partial}{\partial r}\left(r\frac{\partial T}{\partial r}\right) \tag{5}$$

$$iT_s = \frac{\alpha_{s,0}}{\omega R_i^2}\frac{1}{r}\frac{\partial}{\partial r}\left(r\frac{\partial T_s}{\partial r}\right) \tag{6}$$

$$p = \rho + T \tag{7}$$

with the radial boundary conditions

$$r = 0: \qquad \frac{\partial T}{\partial r} = 0 \tag{8a}$$

$$\frac{\partial u}{\partial r} = 0 \tag{8b}$$

$$r = 1: \qquad u = 0 \tag{9a}$$

$$T = T_s \tag{9b}$$

$$k_0\frac{\partial T}{\partial r} = k_{s,0}\frac{\partial T_s}{\partial r} \tag{9c}$$

$$r = \Delta = \frac{R_o}{R_i}: \qquad \frac{\partial T_s}{\partial r} = 0 \tag{10}$$

where we have omitted the subscripts 1 in the dimensionless first-order quantities such as density, pressure, velocity, and temperatures. The coefficients ν_0, α_0, and $\alpha_{s,0}$ in Eqs. (4–6) are the kinematic viscosity and thermal diffusivities of the fluid and the solid evaluated at the temperature $T_0(x)$, respectively. Note that $\partial p/\partial x = \partial p(x, t)/\partial x$ in Eq. (4) and $\mathrm{d}T_0(x)/\mathrm{d}x$ in Eq. (5), both of which are independent of r, the radial coordinate.

Momentum Transport

The solution of Eq. (4) subjected to the boundary conditions Eqs. (8b–9a) is

$$u = \frac{ai}{\omega L\gamma}\frac{\partial p}{\partial x}\left[1 - \frac{J_0(\eta)}{J_0(\eta_0)}\right] \tag{11}$$

where $\eta = \eta_0 r$ with $\eta_0 = (i-1)(R_i/\delta_\nu)$ in which $\delta_\nu = (2\nu_0/\omega)^{1/2}$ is the fluid's viscous penetration depth, and $J_0(\eta)$ is the Bessel function of the first kind of order zero. Note that the fluid's viscous penetration depth δ_ν depends on $T_0(x)$ or axial position because the viscosity ν_0 depends on $T_0(x)$. The dimensional form of Eq. (11) was given earlier by Rott[3,4] and Xiao.[6]

We now define cross-sectional average quantities as

$$\bar{\Omega}(x, t) = \frac{1}{A_0}\int_{A_0}\Omega(x, r, t)\,\mathrm{d}A$$

where Ω is any physical quantity and A_0 is cross-sectional area. An area integration of Eq. (11) leads to

$$\bar{u} = \left[1 - \frac{2}{\eta_0}\frac{J_1(\eta_0)}{J_0(\eta_0)}\right]\frac{ai}{\omega L\gamma}\frac{\partial p}{\partial x} \tag{12}$$

where $J_1(\eta_0)$ is the Bessel function of the first kind of order one. Equation (12) indicates that the cross-sectional averaged velocity in a tube is proportional to the pressure gradient, which suggests that it is convenient to express the relationship between the cross-sectional averaged velocity and the axial pressure gradient by introducing a friction factor for a compressible oscillating flow in a tube. This friction factor f can be expressed as

$$\frac{1}{f} = \frac{2i}{\eta_0}\frac{J_1(\eta_0)}{J_0(\eta_0)} - i \tag{13}$$

Consequently, Eq. (12) can be rewritten as

$$\frac{\partial p}{\partial x} = -f\frac{\omega L\gamma}{a}\bar{u} \tag{14}$$

The minus sign on the right-hand side in Eq. (14) is to keep the form similar to that of the steady unidimensional flow in which the direction of velocity in a tube is opposite to that of pressure gradient.

The friction factor f, given in Eq. (13), shows that it depends only on the dimensionless quantity $\eta_0 = (i-1)(R_i/\delta_\nu)$ or a real dimensionless quantity R_i/δ_ν. Note that, for a fixed inner radius, the

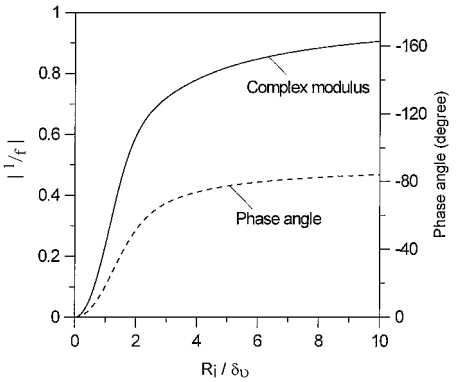

Fig. 2 Variation of $1/f$ with respect to R_i/δ_ν.

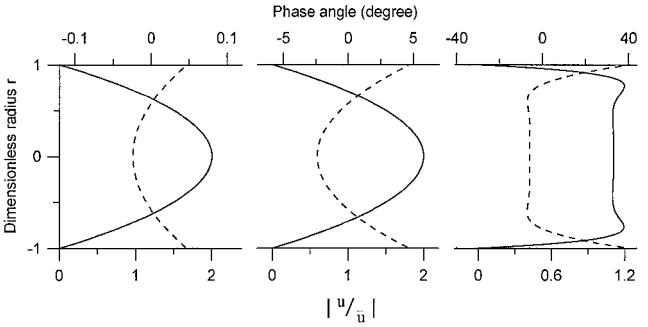

Fig. 3 Relative amplitudes and phase angles of velocities at different values of R_i/δ_ν: ——, complex modulus, and - - - -, phase angle.

friction factor f depends on the local cycle-average temperature because the fluid's viscous penetration depth δ_ν depends on the local cycle-average temperature. The friction factor f in Eq. (13) is a complex number, which indicates that there is a phase shift between the pressure gradient and the cycle-average velocity due to the transient term in Eq. (4). Thus, the friction factor of a compressible flow oscillating at a high frequency depends on the local cycle-average temperature and subject to a phase shift between the velocity and pressure gradient. These characteristics are different from those of a steady unidirectional incompressible flow.

The variation of the reciprocal of friction factor f with respect to R_i/δ_ν is shown in Fig. 2. The reason for plotting a graph of $1/f$ vs R_i/δ_ν instead of f vs R_i/δ_ν is to avoid an infinite value of f when R_i/δ_ν approaches zero so that the vertical coordinate in Fig. 2 is finite. From Fig. 2, we can see that when R_i/δ_ν approaches zero, the complex modulus and phase angle of $1/f$ also approach zero. In other words, the complex modulus of the friction factor f approaches to an infinite value while its phase angle approaches to zero. Physically, if the inner diameter R_i of the tube is too narrow, that is, far smaller than the fluid's viscous penetration depth δ_ν, then the flow cannot penetrate it. Another possible case is the fluid's viscous penetration depth δ_ν is too thick, and the flow also cannot penetrate it due to the large viscosity. It is also shown in Fig. 2 that the values of $1/f$ are almost independent of R_i/δ_ν when $R_i/\delta_\nu \gg 1$, which seems to be reasonable because the viscous effect can be neglected for the flow in a tube with inner radius much larger than the fluid's viscous penetration depth δ_ν. The limiting case is

$$\lim_{\eta_0 \to \infty} (1/f) = -i$$

which implies that the pressure gradient has a phase lag of 90 deg from that of cross-sectional average velocity when $R_i/\delta_\nu \gg 1$ according to Eq. (14). Additionally, Fig. 2 also shows that the phase angle of $1/f$ ranges from 0 to -90 deg for any value of R_i/δ_ν; therefore, the phase angle of friction factor f ranges from 0 to 90 deg, which indicates the range of phase shift between the pressure gradient and cross-sectional average velocity is from 180 to 270 deg according to Eq. (14).

To understand the momentum transport characteristic further, it is useful to present the radial velocity profiles in a graphical form. From Eqs. (11) and (12), we have

$$\frac{u}{\bar{u}} = \left[1 - \frac{J_0(\eta)}{J_0(\eta_0)}\right] \Bigg/ \left[1 - \frac{2}{\eta_0}\frac{J_1(\eta_0)}{J_0(\eta_0)}\right] = \left|\frac{u}{\bar{u}}\right| e^{i\vartheta_r} \tag{15}$$

The complex modulus $|u/\bar{u}|$ and phase angles ϑ_r for different values of R_i/δ_ν are presented in Fig. 3. It is shown that the oscillating amplitudes and phase differences of axial velocity at the different radial locations with respect to those of cross-sectional average velocity are different. This is because the shape of the velocity profile is influenced by the inertia force, pressure gradient, and viscous force. Consider the case of $R_i/\delta_\nu \ll 1$, that is, the case where the inner radius of the tube is much smaller than the fluid's viscous penetration depth, such as the flow in a regenerator, which may be referred to as flow in a narrow tube. As shown in Fig. 3a, one can find that the phase shift for this case is very small, approaching zero, and the complex modulus appears as a parabolic curve. The case of $R_i/\delta_\nu \gg 1$ corresponding to the case where the inner radius of the tube is much larger than the fluid's viscous penetration depth, which may be referred to flow in a tube with a large diameter, such as a resonant tube in a thermoacoustic refrigerator or a pulse tube in a pulse-tube refrigerator. As shown in Fig. 3c, one can see that the velocity overshoot appears near the wall in this case. It is also shown that the effect of viscosity in the tube is confined within a thin layer, and the flow in the main domain appears to be a plug flow. It is shown that the phase angle of the flow near the wall is more advanced than that of the flow near the centerline of the tube in Fig. 3.

Dimensionless axial velocity variations with respect to time are shown in Fig. 4, where the vertical coordinate is for the axial velocity and the horizontal coordinate is for the radial position. The value of the axial velocity is scaled as $\Re(u)/|\bar{u}| = \Re(U_d e^{i\omega t + i\vartheta_r})/|\bar{u}| = |u/\bar{u}|\cos(\omega t + \vartheta_r)$, where $\Re$ is the real part and ϑ_r is the phase angle, and the values of amplitude $|u/\bar{u}|$ and phase angle ϑ_r are presented in Fig. 3.

Energy Transport

The interfacial heat transfer coefficient h between the solid phase and the oscillating flow in a tube is defined as

$$h = \frac{k(\partial T^*/\partial r^*)_{r^* = R_i}}{\bar{T}_s^* - \bar{T}^*} = \frac{k_0}{R_i}\frac{(\partial T/\partial r)_{r=1}}{\bar{T}_s - \bar{T}} \tag{16}$$

where $\bar{T}_s$ and $\bar{T}$ are the cross-sectional averaged temperatures of the solid phase and the oscillating flow, respectively. A cross-sectional averaging of Eqs. (5) and (6) leads to

$$i\bar{T} + \frac{a}{\omega L}\frac{1}{T_0}\frac{\mathrm{d}T_0}{\mathrm{d}x}\bar{u} = \frac{\gamma - 1}{\gamma} ip + \frac{2\alpha_0}{\omega R_i^2}\left(\frac{\partial T}{\partial r}\right)_{r=1} \tag{17}$$

$$i\bar{T}_s = -\frac{2\alpha_{s,0}}{\omega\left(R_o^2 - R_i^2\right)}\left(\frac{\partial T_s}{\partial r}\right)_{r=1} = -\frac{2\alpha_{s,0}}{\omega\left(R_o^2 - R_i^2\right)}\frac{k_0}{k_{s,0}}\left(\frac{\partial T}{\partial r}\right)_{r=1} \tag{18}$$

where we have used the boundary condition of Eq. (9c) and Eq. (10) in Eq. (18). Define Nusselt number $Nu = 2hR_i/k_0$ and substitute Eqs. (17) and (18) in Eq. (16) to give

$$\frac{1}{Nu} = \frac{i\alpha_{s,0}}{\omega\left(R_o^2 - R_i^2\right)}\frac{k_0}{k_{s,0}} + \frac{i\alpha_0}{\omega R_i^2} - \left(\frac{\gamma - 1}{2\gamma} p + \frac{ia}{\omega L}\frac{1}{T_0}\frac{\mathrm{d}T_0}{\mathrm{d}x}\bar{u}\right) \Bigg/ \left(\frac{\partial T}{\partial r}\right)_{r=1} \tag{19}$$

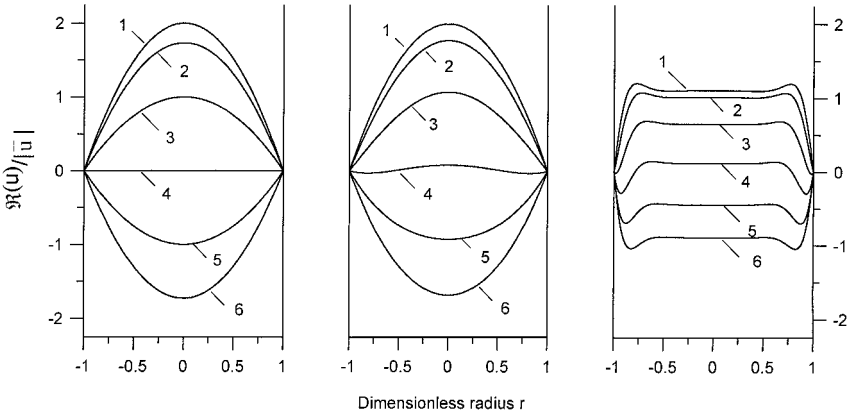

Fig. 4 Velocity variations with respect to time at different values of R_i/δ_ν: 1, $\omega t = 0$; 2, $\omega t = \pi/6$; 3, $\omega t = \pi/3$; 4, $\omega t = \pi/2$; 5, $\omega t = 2\pi/3$; and 6, $\omega t = 5\pi/6$.

To determine $(\partial T/\partial r)_{r=1}$, we now return our attention to Eqs. (3–10), which can be solved to give

$$T = \left[\frac{b_1}{1-\sigma^2}\frac{J_0(\sigma\eta)}{J_0(\sigma\eta_0)} - \frac{\sigma^2}{1-\sigma^2}\frac{J_0(\eta)}{J_0(\eta_0)} - 1\right]\frac{1}{\gamma}\left(\frac{a}{\omega L}\right)^2 \times \frac{\partial p}{\partial x}\frac{1}{T_0}\frac{\mathrm{d}T_0}{\mathrm{d}x} + \left[1 - \frac{1}{1-b_2}\frac{J_0(\sigma\eta)}{J_0(\sigma\eta_0)}\right]\frac{\gamma-1}{\gamma}p \tag{20}$$

where coefficients b_1 and b_2 are given as follows:

$$b_1 = \left\{\frac{\sigma J_1(\eta_0)}{J_0(\eta_0)}\left[\frac{Y_1(\sigma_s\Delta\eta_0)}{J_1(\sigma_s\Delta\eta_0)} - \frac{Y_0(\sigma_s\eta_0)}{J_0(\sigma_s\eta_0)}\right] - \varepsilon\frac{J_1(\sigma_s\eta_0)}{J_0(\sigma_s\eta_0)}\left[\frac{Y_1(\sigma_s\Delta\eta_0)}{J_1(\sigma_s\Delta\eta_0)} - \frac{Y_1(\sigma_s\eta_0)}{J_1(\sigma_s\eta_0)}\right]\right\}\Bigg/ \left\{\frac{J_1(\sigma\eta_0)}{J_0(\sigma\eta_0)}\left[\frac{Y_1(\sigma_s\Delta\eta_0)}{J_1(\sigma_s\Delta\eta_0)} - \frac{Y_0(\sigma_s\eta_0)}{J_0(\sigma_s\eta_0)}\right] - \varepsilon\frac{J_1(\sigma_s\eta_0)}{J_0(\sigma_s\eta_0)}\left[\frac{Y_1(\sigma_s\Delta\eta_0)}{J_1(\sigma_s\Delta\eta_0)} - \frac{Y_1(\sigma_s\eta_0)}{J_1(\sigma_s\eta_0)}\right]\right\} \tag{21}$$

$$b_2 = \frac{1}{\varepsilon}\left\{\frac{J_1(\sigma\eta_0)}{J_0(\sigma\eta_0)}\left[\frac{Y_1(\sigma_s\Delta\eta_0)}{J_1(\sigma_s\Delta\eta_0)} - \frac{Y_0(\sigma_s\eta_0)}{J_0(\sigma_s\eta_0)}\right]\Bigg/ \frac{J_1(\sigma_s\eta_0)}{J_0(\sigma_s\eta_0)}\left[\frac{Y_1(\sigma_s\Delta\eta_0)}{J_1(\sigma_s\Delta\eta_0)} - \frac{Y_1(\sigma_s\eta_0)}{J_1(\sigma_s\eta_0)}\right]\right\} \tag{22}$$

with $\sigma = (\nu_0/\alpha_0)^{1/2} = Pr^{1/2}$, $\sigma_s = (\nu_0/\alpha_{s,0})^{1/2}$, and $\varepsilon = k_{s,0}\sigma_s/k_0\sigma$. Note that dimensionless quantities σ, σ_s, and ε are thermal property parameters that depend on local temperature $T_0(x)$. The temperature distribution given by Eqs. (20–22) are much simpler in form than those dimensional solutions obtained by Xiao[6] for the special case where the outside of the tube is thermally insulated. An integration of Eq. (20) across the cross-sectional area leads to

$$\bar{T} = \left[\frac{b_1}{1-\sigma^2}\frac{2}{\sigma\eta_0}\frac{J_1(\sigma\eta_0)}{J_0(\sigma\eta_0)} - \frac{\sigma^2}{1-\sigma^2}\frac{2}{\eta_0}\frac{J_1(\eta_0)}{J_0(\eta_0)} - 1\right]\frac{1}{\gamma}\left(\frac{a}{\omega L}\right)^2 \times \frac{\partial p}{\partial x}\frac{1}{T_0}\frac{\mathrm{d}T_0}{\mathrm{d}x} + \left[1 - \frac{1}{1-b_2}\frac{2}{\sigma\eta_0}\frac{J_1(\sigma\eta_0)}{J_0(\sigma\eta_0)}\right]\frac{\gamma-1}{\gamma}p \tag{23}$$

where $\bar{T}$ is the cross-sectional average temperature. Equation (23) indicates that the fluctuation of local mean temperature consists of two parts: The first term is due to local cycle-steady temperature gradient and local pressure gradient, whereas the second term is due to local pressure fluctuation. The dimensionless temperature distribution is given by

$$\frac{T}{\bar{T}} = \left\{\left[\frac{b_1}{1-\sigma^2}\frac{J_0(\sigma\eta)}{J_0(\sigma\eta_0)} - \frac{\sigma^2}{1-\sigma^2}\frac{J_0(\eta)}{J_0(\eta_0)} - 1\right]\phi + \left[1 - \frac{1}{1-b_2}\frac{J_0(\sigma\eta)}{J_0(\sigma\eta_0)}\right](\gamma-1)\right\}\Bigg/ \left\{\left[\frac{b_1}{1-\sigma^2}\frac{2}{\sigma\eta_0}\frac{J_1(\sigma\eta_0)}{J_0(\sigma\eta_0)} - \frac{\sigma^2}{1-\sigma^2}\frac{2}{\eta_0}\frac{J_1(\eta_0)}{J_0(\eta_0)} - 1\right]\phi + \left[1 - \frac{1}{1-b_2}\frac{2}{\sigma\eta_0}\frac{J_1(\sigma\eta_0)}{J_0(\sigma\eta_0)}\right](\gamma-1)\right\} \tag{24}$$

where dimensionless quantity

$$\phi = \left(\frac{a}{\omega L}\right)^2 \frac{1}{T_0}\frac{\mathrm{d}T_0}{\mathrm{d}x}\frac{1}{p}\frac{\partial p}{\partial x}$$

depends only on axial location x and is independent of time for a fixed operation condition. This is because, under the harmonic assumption,

$$\frac{1}{p}\frac{\partial p}{\partial x} = \frac{1}{p_d e^{i\omega t + i\vartheta}}\frac{\partial\left(p_d e^{i\omega t + i\vartheta}\right)}{\partial x} = \frac{1}{p_d e^{i\vartheta}}\frac{\partial\left(p_d e^{i\vartheta}\right)}{\partial x}$$

where p_d is the oscillating amplitude of the pressure that depends on axial location and is independent of time. Note that the sign of the dimensionless quantity ϕ depends on the local pressure and the local temperature gradients.

Equation (24) was computed for different values of R_i/δ_ν under the following conditions:

1) The fluid is helium gas, and the tube is made of stainless steel.

2) Mean working pressure is $p_0 = 1$ MPa, and at a local zero-order temperature, $T_0 = 80$ K.

3) The geometrical parameter Δ is assumed to be equal to 1.12, which is related to porosity of the porous medium if the porous medium is considered to be a bundle of capillary tubes.

Under these conditions and with the thermal properties given by Scott,[11] the dimensionless parameters are given by $\sigma = 0.876$, $\sigma_s = 0.447$, $\varepsilon = 86.469$, and $\gamma = 1.667$. Figure 5 shows distributions of relative amplitudes and phase angles of temperatures at different radial locations for different R_i/δ_ν at $\phi = 1$. For the case of $\phi = -1$, distributions of amplitude and phase angle are similar to Fig. 5 if the other conditions are identical. Physical meanings of complex modulus and phase angles of the dimensionless temperature presented in Fig. 5 are similar to those of the dimensionless velocity distributions discussed earlier. For the case of $R_i/\delta_\nu = 1$, as shown in Fig. 5c, the complex modulus appears to be of a parabolic shape; its profile is similar to that of the velocity (see Fig. 3), and there are phase shifts at different radial locations. For the case of $R_i/\delta_\nu \ll 1$, as shown in Fig. 5a, the complex moduli of the axial velocity have almost the

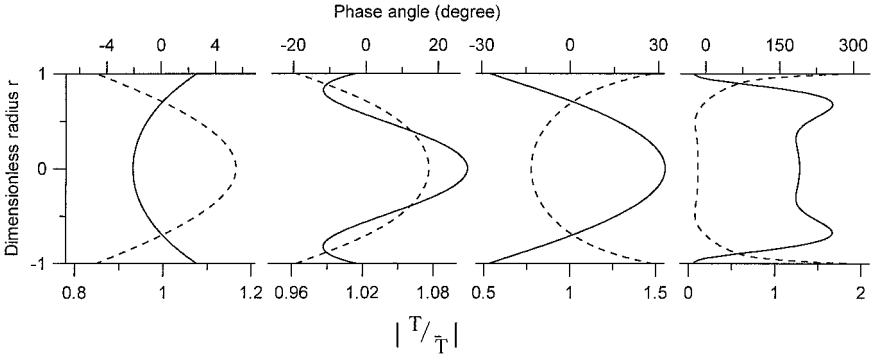

Fig. 5 Relative amplitudes and phase angles of temperature for different values of R_i/δ_ν: ——, complex modulus, and - - - -, phase angle.

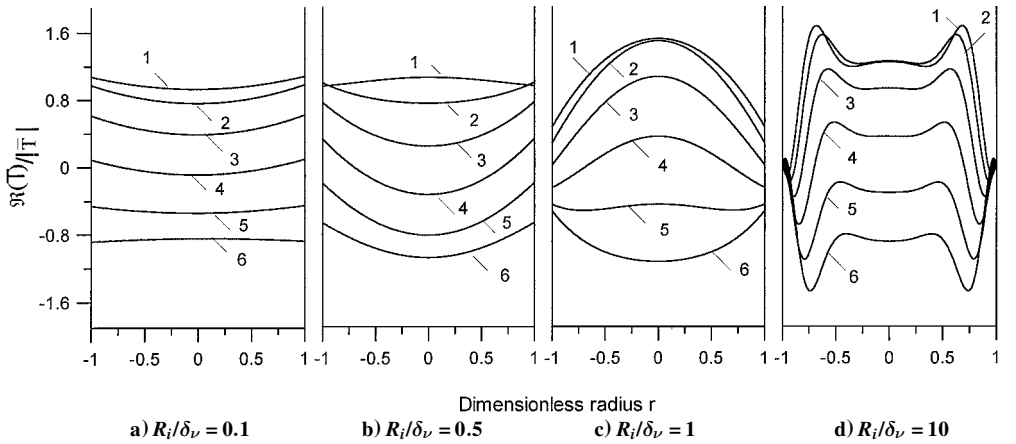

Fig. 6 Temperature variations with respect to time for different values of R_i/δ_ν at $\phi = 1$: 1, $\omega t = 0$; 2, $\omega t = \pi/6$; 3, $\omega t = \pi/3$; 4, $\omega t = \pi/2$; 5, $\omega t = 2\pi/3$; and 6, $\omega t = 5\pi/6$.

same value, whereas differences in phase angle are very small. Mathematically, it can be shown that $\lim_{\eta_0 \to 0} (T/\bar{T}) = 1$, which indicates that oscillating amplitudes at different radial locations approach an identical value with radial differences of phase angles approaching zero degree when $R_i/\delta_\nu \ll 1$. Nevertheless, there are still small deviations of amplitude and phase angle from their limits as shown in Fig. 5a. Mathematically, it can be shown that the first braced term in the numerator in Eq. (24) approaches zero while the second braced term in the numerator in Eq. (24) dominates the temperature profile when $R_i/\delta_\nu \ll 1$, which leads to the conclusion that the local temperature variations in Eq. (20) during a cycle in this case are almost independent of local cycle-steady temperature gradient and local pressure gradient while they mainly depend on local pressure variations. Figure 5a also shows that the oscillating amplitude of the temperature near the wall is larger than that near the centerline, which is different from the velocity profile as shown in Fig. 3a. This is due to the interaction between the solid phase and the fluid phase that affects the value of coefficients b_2 in Eq. (24). The flow in the tube in this case can be considered as a highly viscous flow, and the interaction between the solid phase and the fluid phase has an important role on the temperature profile. As the value of R_i/δ_ν is increased from 0.5 to 1.0, as shown in Figs. 5b and 5c, the importance of the wall on the temperature of the fluid becomes weaker, and the temperature profile at the center becomes a parabolic shape similar to that of velocity. For the case of $R_i/\delta_\nu \gg 1$, as shown in Fig. 5d, it can be seen that the temperature oscillating amplitude near the wall is small, and there is temperature overshoot near the wall while it appears to be a plug flow near the centerline. This indicates that the effect of thermal condition of the wall on the temperature profile of the fluid is also confined in a thin layer, and its shape is very similar to the velocity profile. Note that the overshoot of the temperature profile is similar to that of velocity as shown in Fig. 3c. To give physical insight to the problem, temperature variations with respect to time are presented in Fig. 6. For the case of $R_i/\delta_\nu \ll 1$, as shown in Fig. 6a, temperature variations with respect to radial locations are very small, that is, temperature is independent of radial locations.

We now return our attention to the Nusselt number. Substituting Eqs. (12) and (20) in Eq. (19) and recalling the definitions of dimensionless quantities ε, σ, σ_s, Δ, and η_0, we have

$$\frac{1}{Nu} = \left\{ \frac{\gamma - 1}{2} - \left[\frac{1}{2} - \frac{1}{\eta_0} \frac{J_1(\eta_0)}{J_0(\eta_0)} \right] \phi \right\} \Bigg/ \left\{ \frac{\sigma\eta_0}{1-\sigma^2} \left[b_1 \frac{J_1(\sigma\eta_0)}{J_0(\sigma\eta_0)} - \sigma \frac{J_1(\eta_0)}{J_0(\eta_0)} \right] \phi - \left(\frac{\gamma - 1}{1 - b_2} \right) \frac{\sigma\eta_0 J_1(\sigma\eta_0)}{J_0(\sigma\eta_0)} \right\} + \frac{1}{\varepsilon\sigma\sigma_s(\Delta^2 - 1)\eta_0^2} + \frac{1}{\sigma^2\eta_0^2} \tag{25}$$

which shows that the Nusselt number is a complex number indicating that there is a phase shift between the heat flux and the temperature difference of the wall and the oscillating flow. Equation (25) also shows that the Nusselt number depends on thermal property parameters σ, σ_s, ε, and γ, the geometrical parameter Δ, and operation conditions parameters η_0 and ϕ. For a certain system with given geometrical size and oscillating frequency of a specific working fluid, Eq. (25) shows that the Nusselt number depends only on axial position and is independent of time. This is because thermal property parameters and η_0 depend only on cycle-steady axial temperature as a result of the linearization of the governing equations, whereas ϕ depends only on axial position as we had discussed earlier. In Eq. (25), we express the reciprocal of Nusselt number Nu for simplicity. When the right side of Eq. (25) approaches to zero, Nusselt number will approach an infinite complex value, which indicates that $\bar{T}_s = \bar{T}$ at this singularity point.

Figure 7 shows the variations of Nusselt number with respect to the dimensionless quantity ϕ when $R_i/\delta_\nu = 1$, which were

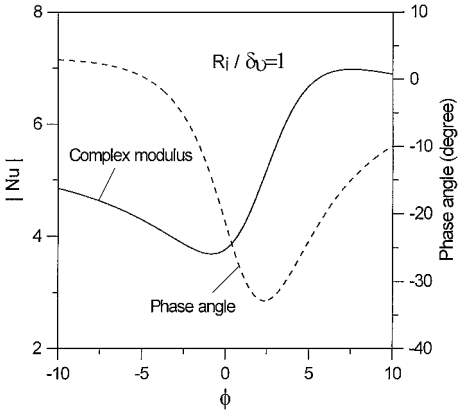

Fig. 7 Variation of Nusselt number with respect to dimensionless quantity ϕ.

calculated based on the same conditions as in Figs. 5 and 6. In Fig. 7, the complex modulus indicates the oscillating amplitude of Nusselt number, whereas the phase angle indicates that there is phase shift between heat flux and temperature difference of the solid and the oscillating fluid. Consider first the case where the flow has a negative pressure gradient. The positive side of ϕ in Fig. 7 corresponds to the case having a negative temperature gradient such as in a regenerator of the thermoacoustic machine, whereas the negative side of ϕ in Fig. 7 is for the case having a positive temperature gradient such as in the pulse tube of a Stirling-type pulse-tube refrigerator. If the flow has a positive pressure gradient, the positive side of ϕ would correspond to a positive temperature gradient whereas the negative side of ϕ would correspond to a negative temperature gradient.

We now discuss the Nusselt numbers for the limiting cases of 1) $R_i/\delta_v \ll 1$ and 2) $R_i/\delta_v \gg 1$ by examining the asymptotic behaviors of Eq. (25). As discussed before, the first case corresponds to the flow in a narrow tube, whereas the second case may be applied to the flow in a tube with a large diameter.

1) At the limiting case of $\eta_0 \to 0$:

$$\lim_{\eta_0 \to 0} b_1 = 1, \qquad \lim_{\eta_0 \to 0} b_2 = \frac{1}{\varepsilon}\frac{\sigma}{\sigma_s}\frac{1}{1-\Delta^2} \tag{26}$$

$$\lim_{\eta_0 \to 0} \frac{\eta_0^2}{Nu} = 1 \Bigg/ \left[\frac{\sigma}{1+\sigma}\frac{1}{\gamma-1}\phi - \frac{\varepsilon\sigma\sigma_s(\Delta^2-1)}{\varepsilon\sigma_s(\Delta^2-1)+\sigma}\right] + \frac{1}{\varepsilon\sigma\sigma_s(\Delta^2-1)} + \frac{1}{\sigma^2} \tag{27}$$

In Eqs. (26) and (27), we have used the limit of

$$\lim_{\eta_0 \to 0} \frac{J_1(\eta_0)}{\eta_0 J_0(\eta_0)} = 0.5$$

and the limiting values of $Y_0(\eta_0)$ and $Y_1(\eta_0)$. It can be seen from Eq. (27) that Nusselt number is the same order as η_0^2 when $R_i/\delta_v \ll 1$.

2) At the limiting case of $\eta_0 \to \infty$:

$$\lim_{\eta_0 \to \infty} b_1 = \frac{\sigma-\varepsilon}{1-\varepsilon}, \qquad \lim_{\eta_0 \to \infty} b_2 = \frac{1}{\varepsilon} \tag{28}$$

$$\lim_{\eta_0 \to \infty} \frac{\eta_0}{Nu} = \frac{i(\varepsilon-1)}{2\varepsilon\sigma}\left[\frac{\phi-\gamma+1}{\phi/(1+\sigma)+\gamma-1}\right] + \frac{1}{\varepsilon\sigma\sigma_s(\Delta^2-1)\eta_0} + \frac{1}{\sigma^2\eta_0} \tag{29}$$

It can be seen from Eq. (29) that Nusselt number is the same order as η_0 when $R_i/\delta_v \gg 1$. Note that the last two terms at the right-hand side of the Eq. (29) will also approach zero when η_0 approaches infinity.

Discussion

In the preceding paragraphs, we have introduced complex numbers to analyze the transport phenomena in an oscillatory flow. We represent temperature, pressure, velocity, or density, in the form of $\Omega = \Omega_0 + \Omega_d e^{i\omega t + i\vartheta}$, in which Ω_0 indicates the cycle-average value, Ω_d indicates amplitude, and ϑ indicates phase angle. Note that only the real part of Ω has physical meaning, which varies with respect to time and locations. However, the dimensionless velocity distribution $u/\bar{u}$ given by Eq. (15) and the dimensionless temperature distribution $T/\bar{T}$ given by Eq. (24) have physical significance in both real and imaginary parts. For an oscillatory flow, the friction factor and Nusselt number also have physical significance in both real and imaginary parts. To illustrate this point, we now take Nusselt number as an example. Traditionally, the Nusselt number is defined as

$$Nu \propto \frac{(\partial T/\partial r)_{r=1}}{\bar{T}_s - \bar{T}} \tag{30a}$$

If the real parts of T and T_s are substituted into expression (30a), we have

$$Nu \propto \frac{(\partial T/\partial r)_{r=1}}{\bar{T}_s - \bar{T}} = \frac{\{(\partial/\partial r)[T_d \cos(\omega t + \vartheta)]\}_{r=1}}{\overline{T_{s,d}\cos(\omega t + \vartheta_s)} - \overline{T_d \cos(\omega t + \vartheta)}} \tag{30b}$$

where it is difficult to obtain a correlation equation due to its time-dependent characteristic of physical quantities.

By the introduction of the complex algorithm, Eq. (30a) gives

$$Nu \propto \frac{(\partial T/\partial r)_{r=1}}{\bar{T}_s - \bar{T}} = \frac{\left[(\partial/\partial r)\left(T_d e^{i(\omega t+\vartheta)}\right)\right]_{r=1}}{\overline{T_{s,d}e^{i(\omega t+\vartheta_s)}} - \overline{T_d e^{i(\omega t+\vartheta)}}} = \frac{\left[(\partial/\partial r)\left(T_d e^{i\vartheta}\right)\right]_{r=1}}{\overline{T_{s,d}e^{i\vartheta_s}} - \overline{T_d e^{i\vartheta}}} \tag{31}$$

which shows that the Nusselt number is independent of time. Therefore, the Nusselt number Nu given by Eq. (31) gives the relationships of amplitudes and phase angles between heat flux and temperature difference. However, note that its real part does not correspond to the traditional defined Nusselt number as described in Eq. (30b). Note that the physical meaning of the complex modulus and the phase angle of the friction factor are similar to those of the Nusselt number as discussed in this section.

Conclusions

We have obtained analytical solutions based on the first-order linearized equations for the friction factor and the Nusselt number of a viscous compressible flow oscillating at high frequencies in a tube subjected to a cycle-steady axial temperature gradient. Particular attention has been given to the transport phenomena for the asymptotic cases of $R_i/\delta_v \ll 1$ and $R_i/\delta_v \ll 1$. The former corresponds to a tube with a small diameter (such as in the flow of porous medium in the regenerator) whereas the latter corresponds to a tube with a large diameter (such as a resonant tube of the thermoacoustic refrigerator or a pulse tube of the Stirling-type pulse-tube refrigerator). The results can be summarized as follows:

1) By solving the momentum equation, we found that there are phase shifts for axial velocities at different radial locations compared to cross-sectional averaged axial velocity in a tube. When $R_i/\delta_v \ll 1$, phase shifts are very small (approaching zero in the limit), and the complex modulus of velocity (normalized with respect to the cross-sectional axial averaged velocity) appears to be of parabolic shape. When $R_i/\delta_v \gg 1$, the viscosity effects in the tube are confined within a thin layer with velocity overshoot occurring near the wall, and the flow in main domain appears almost as a plug flow. The friction factor of a viscous compressible oscillating flow in a tube has

been theoretically determined. It is shown that the friction factor depends on the axial cycle-steady temperature and is a complex number because of the phase shift between the cross-sectional average velocity and pressure gradient. These characteristics differ from that of steady unidirectional viscous incompressible flow in a tube.

2) By solving the energy equations of the fluid and solid phases, a closed-form analytical solution for the temperature distribution in the fluid is obtained. When $R_i/\delta_\nu \ll 1$, oscillating amplitudes of temperature have an almost uniform profile, which is independent of radial locations and the phase angles in different radial positions approach to a zero degree. In this case, the flow in the tube can be considered as a highly viscous flow, and the interaction between the solid phase and the fluid phase has an important role on the temperature profile. For the case of $R_i/\delta_\nu \gg 1$, it is shown that the effect of solid/fluid interaction on the temperature profile is confined in a thin layer, similar to the velocity profile. There is overshoot in the temperature profiles, which are similar to those of velocity profiles. The interaction of the thermal condition of the wall on the temperature of the fluid can be neglected at the region near the centerline, which shows a flat profile. A closed-form analytical solution for the interfacial Nusselt number has been obtained. It is shown that the Nusselt number is also a complex number, which indicates there is a phase shift between the wall heat flux and the temperature difference between the wall and the oscillating flow. The Nusselt number is shown to be dependent on thermal property parameters σ, σ_s, ε, and γ, the geometrical parameter Δ, and operation conditions parameters η_0 and ϕ, and its value depends on the axial position and it is independent of time. Two limiting cases of the Nusselt number have been discussed, and the result show that the Nusselt number is the same order as η_0^2 when $R_i/\delta_\nu \ll 1$, whereas the Nusselt number is the same order as η_0 when $R_i/\delta_\nu \gg 1$.

Acknowledgments

This work was supported by Research Grants Council, under Grants HKUST 709/95E and HKUST6039/99E.

References

[1]Swift, G. W., "Analysis and Performance of a Large Thermoacoustic Engine," *Journal of Acoustical Society of America*, Vol. 92, No. 3, 1992, pp. 1551–1563.

[2]Garrett, S. L., Adeff, J. A., and Holfer, T. J., "Thermoacoustic Refrigerator for Space Applications," *Journal of Thermophysics and Heat Transfer*, Vol. 7, No. 4, 1993, pp. 595–599.

[3]Rott, N., "Damped and Thermally Driven Acoustic Oscillations in Wide and Narrow Tubes," *Journal of Applied Mathematics and Physics*, Vol. 20, No. 2, 1969, pp. 230–243.

[4]Rott, N., "Thermoacoustics," *Advances in Applied Mechanics*, Vol. 20, 1980, pp. 135–175.

[5]Swift, G. W., "Thermoacoustic Engines," *Journal of the Acoustical Society of America*, Vol. 84, No. 4, 1988, pp. 1145–1180.

[6]Xiao, J. H., "Thermoacoustic Heat Transport and Energy Transformations, Part 1: Formulation of the Problem," *Cryogenics*, Vol. 35, No. 1, 1995, pp. 15–19.

[7]Kays, W. M., and London, A. L., *Compact Heat Exchangers*, 3rd ed., McGraw–Hill, New York, 1984, pp. 148, 149.

[8]Tanaka, M., Yamashita, I., and Chisaka, F., "Flow and Heat Transfer Characteristics of the Stirling Engine Regenerator in an Oscillating Flow," *Japan Society of Mechanical Engineers International Journal, Series II*, Vol. 33, No. 2, 1990, pp. 283–289.

[9]Watanabe, M., Prosperetti, A., and Yuan H., "A Simplified Model for Linear and Nonlinear Processes in Thermoacoustic Prime Movers, Part I: Model and Linear Theory," *Journal of the Acoustical Society of America*, Vol. 102, No. 6, 1997, pp. 3484–3496.

[10]Bauwens, L., "Oscillating Flow of a Heat-Conducting Fluid in a Narrow Tube," *Journal of Fluid Mechanics*, Vol. 324, Oct. 1996, pp. 135–161.

[11]Scott, R. B., *Cryogenic Engineering*, Met-Chen Research, Inc., Boulder, CO, 1988, pp. 267–350.